Performance of M-ary PPM UWB Radio in Fading Channels

Mohammed Abdel-Hafez, Fatih Alagöz, and Matti Hämäläinen

Abstract: **This paper investigates the performance of M-ary pulse position modulation (PPM) multiuser ultra-wideband (UWB) communication systems in terms of symbol error rate (SER) over fading and additive white Gaussian noise (AWGN) channel. Based on Gaussian approximation for the multiple access interference, an expression for the signal-to-noise ratio (SNR) is derived for the UWB system. This expression is used to derive exact SER expressions for coherent UWB receivers. The effect of pulse selection on the SER of multiuser UWB system is studied. In addition to rectangular pulse, the 2nd derivative Gaussian waveform and Rayleigh pulses were considered. We show that the system capacity and/or SER performance can be significantly increased by using the monocycle pulse in fading channels.**

Index Terms: **Ultra-wideband communications (UWB), interference, time-hopping, bit-error-rate (BER), fading channels, M-ary PPM modulation.**

I. INTRODUCTION

Ultra-wideband (UWB) systems were recently proposed as one of the possible solutions for short range wireless networks [1]. UWB radio is the generic term describing radio systems having very large bandwidths; "bandwidths greater than 20% of the center frequency measured at the -10dB points," and "RF bandwidth greater than 500 MHz," are the two of the definitions under consideration by the US Federal Communications Commissions (FCC) [2]. This new technology has the potential to deliver high data rates with very low power densities. The UWB systems are characterized by the transmission of series of sub-nanosecond pulses (monocycles) that spread the energy of the signal from near DC to a few GHz. The pulse train is transmitted without any modulation with sinusoidal carrier. This is a major advantage of single band UWB since it has high immunity against multipath fading effect as experienced in other wireless systems. In addition, high processing gain and very low power density ensure minimal mutual interference between the UWB and other wireless systems. Pulse position modulation (PPM) has been proposed as a modulation scheme suitable for the UWB communications [1]. With PPM, the data modulates the position of the transmitted pulse within an assigned window in time.

Manuscript received August 9, 2003.

M. Abdel-Hafez is with Department of Electrical Engineering, United Arab Emirates University, P.O.BOX 17555, Al-Ain, United Arab Emirates, email: mhafez@uaeu.ac.ae.

F. Alagöz is with Department of Electrical and Electronics Engineering, Harran University, Sanliurfa, TURKEY, email: alagoz@harran.edu.tr.

M. Hämäläinen is with Centre for Wireless Communications, University of Oulu, Tutkijantie 2 E, FIN-90570 Oulu, FINLAND, email: matti.hamalainen@ee.oulu.fi.

Time Hopping (TH) is used in the UWB system as a multiple-access method. The PPM scheme is used in TH-mode with pulse transmission instants defined by a pseudo random code. One data bit is spread over multiple pulses to achieve a processing gain due to the pulse repetition. The processing gain is increased by the low duty cycle. The multiple-access interference (MAI) may be the dominant factor on the bit error rate (BER) performance. Some published works considered the BER of UWB system in nonfading multipath channel [3], [4]. The correlation properties and the frequency spectra of UWB pulses are very crucial. The BER of a single user M-ary PPM UWB system was considered for fixed multipath fading channel in [3], and its extension to multiuser UWB is presented in [4]. This paper, an extension of our work presented in [5], differentiates itself from other previous works by introducing the effect of pulse shape and fading on the performance of multiuser UWB system. Rician and Nakagami fading channels have been selected for their generalized modeling of short range UWB channel [6].

The remainder of the paper is organized as follows. Section II introduces the signal, channel, and receiver models. Section III carries out the performance analysis of the UWB M-ary PPM in Gaussian, Rician, and Nakagami fading channels. Section IV presents the numerical results. Section V concludes this study.

II. UWB SYSTEM MODEL

The time-hopping M-ary PPM system model examined in this paper is shown in Fig. 1. The j-th pulse for the v-th user's transmitted signal has the form [1]

$$S_j^{\nu}(t) = A^{\nu} P(t - jT_f - C_j^{\nu} T_C - d_j^{\nu}), \tag{1}$$

and the ν-th user's transmitted signal has the form [1]

$$\begin{aligned} S^{\nu}(t) &= \sum_{j=-\infty}^{\infty} S_j^{\nu}(t) \\ &= \sum_{j=-\infty}^{\infty} A^{\nu} P(t - jT_f - C_j^{\nu} T_C - d_j^{\nu}), \end{aligned} \tag{2}$$

where $P(t)$ is the normalized UWB pulse of duration T_P. The pulse repetition interval, referred to as *frame*, is T_f. The amplitude, user dependent time-hopping code and data modulation for ν-th user are A^{ν}, C_j^{ν} and d_j^{ν}, respectively. The time shift introduced by the PPM modulation is $d_j^{\nu} \in \{\delta_1, \cdots, \delta_M\}$, where δ_i for $1 \leq i \leq M$ is the basic time shift for the i-th M-ary symbol, as shown in Fig. 2. We assume that $\delta_1 < \cdots < \delta_i < \cdots < \delta_M < T_f$. For a fixed T_P, the symbol rate $R_s = 1/(N_P T_f)$ where N_P is the number of pulses that forms one symbol. The symbol duration is then $T_s = N_P T_f$. The spreading ratio is defined by $\beta = T_f / T_P$.

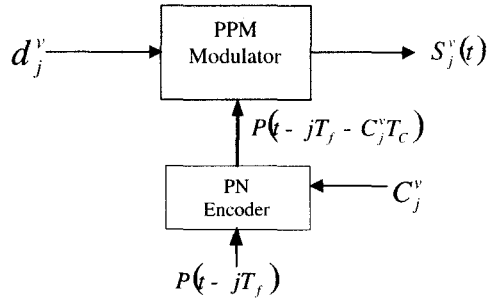

Fig. 1. TH-PPM UWB modulator.

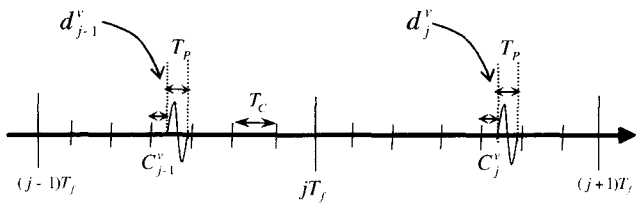

Fig. 2. Example of TH-PPM asynchronous format.

Each user's signal propagates over a single path channel with attenuation factor α and propagation delay τ as shown in Fig. 3. In this study, it is assumed that the channel is a single path Rician channel. The channel is random and its amplitude, α, can be described by Rician distribution. The instantaneous power level, $\gamma = \alpha^2$, follows the non-central Chi-square probability distribution function (*pdf*) as

$$f(\gamma) = \frac{1+K}{\Omega} e^{-\left(\frac{\gamma(1+K)+K\Omega}{\Omega}\right)} I_0\left(2\sqrt{\frac{(1+K)K\gamma}{\Omega}}\right), \quad (3)$$

where Ω is the mean power level, which is equal to the sum of the powers due to the multipath diffused, γ^0_{diff}, and Line-of-Sight (LOS), γ^0_{LOS}, and $I_0(x)$ is the modified Bessel function of the first kind and zero'th order. The Rician distribution is more commonly specified by the Rice factor, K, which is interpreted as the line-of-sight to multipath diffused power ratio, $K = \gamma^0_{LOS}/\gamma^0_{diff}$. The 1st and 2nd moments of α are [9]

$$E[\alpha] = \frac{1}{2}\sqrt{\frac{\Omega\pi}{1+K}} e_1^{-K} F_1\left(\frac{3}{2} : 1; K\right), \quad (4)$$

$$E[\alpha^2] = \Omega = \gamma^0_{LOS} + \gamma^0_{diff}, \quad (5)$$

where $F_1(a : b; x)$ is the confluent Hypergeometric function [7].

If Nakagami channel is assumed, then the random variable α is described by Nakagami distribution [10]. The instantaneous power level $\gamma = \alpha^2$ follows the Gamma *pdf* as

$$f(\gamma) = \frac{1}{\Gamma(m)}\left(\frac{m}{\Omega}\right)^m \gamma^{m-1} \exp\left(-\frac{m}{\Omega}\gamma\right), \; x \geq 0, \quad (6)$$

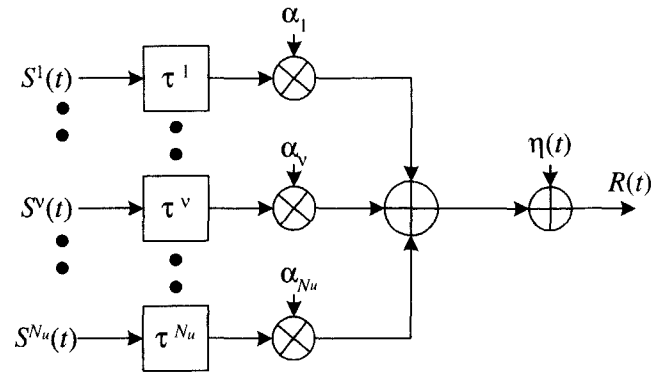

Fig. 3. The channel model.

where Ω is mean power level defined as $\Omega = E[\gamma]$, $\Gamma(m)$ is a gamma function, and $m \in [0.5, \infty)$ is the fading parameter (determines the severity of the fading) defined by $m = \Omega^2/E[(X^2 - \Omega)^2] \geq 1/2$. Less severe fading conditions are modeled by using larger values of the fading parameter m. In the limit when $m \to \infty$, *pdf* of γ tends to a delta function corresponding to the case of nonfading. By setting $m = 1$, we observe that (6) reduces to exponential *pdf*. The n-th moment of α is [9]

$$E[\alpha^2] = \frac{\Gamma(m + \frac{1}{2}n)}{\Gamma(m)}\left(\frac{\Omega}{m}\right)^{\frac{n}{2}}. \quad (7)$$

The Rician distribution can also be closely approximated by Nakagami distribution with $m > 1$. In general, the relationship between the Rice factor K and the fading parameter m [10], is $m = 1/[1 - (\frac{K}{1+K})^2]$. A linear approximation between m and K exists for $K > 2$ [11], $m = 0.4998528K + 0.7622159$.

The received signal $R(t)$ from all users is given by

$$R(t) = \sum_{\nu=1}^{N_u} \alpha_\nu S^\nu(t - \tau^\nu) + \eta(t), \quad (8)$$

where α_ν is the channel attenuation, τ^ν is the time delay associated with user ν (out of total number of N_u users), and $\eta(t)$ is zero-mean AWGN with power spectral density $N_0/2$.

Without loss of generality, we assume that the desired user is $\nu = 1$. The single-user optimal receiver is M-ary pulse correlation receiver followed by a detector. We also assume that the receiver is perfectly synchronized to user 1, i.e., τ^1 is known. Furthermore, the time hopping sequence C_j^1 is known at the receiver. The M-ary correlation receiver for user 1 consists of M filters matched to the basis function $\phi_i^1(t)$ defined as

$$\phi_i^1(t) = P(t - \delta_i - \tau^1), \; i = 1, \cdots, M. \quad (9)$$

The detector selects the Max i-th symbol of M possible outputs, as shown in Fig. 4. The decision variables at time sample $(t = jT_f)$, are now given as

$$U_i = \int_{(j-1)T_f}^{jT_f} R(t)\phi_i^1(t - jT_f - C_j^1 T_C)dt, \quad (10)$$

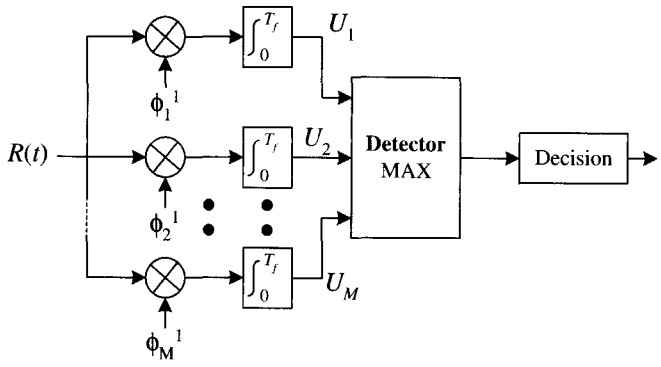

Fig. 4. M-ary PPM UWB receiver for the 1st user.

by substituting for $R(t)$ from (8), the parameter U_i can be represented as

$$U_i = d_i + NI_i + N_i. \tag{11}$$

Without loss of generality, the dependency on i for terms d, NI and N is removed for the rest of the paper. The desired part of the received signal d is expressed as

$$d = \int_{(j-1)T_f}^{jT_f} \alpha_1 S^1(t-\tau^1)\phi_i^1(t - jT_f - C_j^1 T_C)dt. \tag{12}$$

NI is the multiple access interference (MAI) from other users expressed as

$$NI = \int_{(j-1)T_f}^{jT_f} \sum_{\nu=2}^{N_u} \alpha_\nu S^\nu(t-\tau^\nu)\phi_i^1(t - jT_f - C_j^1 T_C)dt. \tag{13}$$

N is the noise component at the output of the receiver,

$$N = \int_{(j-1)T_f}^{jT_f} \eta(t)\phi_i^1(t - jT_f - C_j^1 T_C)dt. \tag{14}$$

Using normalized pulse, the desired part of the signal is expressed as

$$d = \alpha_1 A^1 \delta(d_j^1 - \delta_j), \tag{15}$$

where $\delta(\cdot)$ is the delta function. The MAI part can be written as

$$NI = \sum_{\nu=2}^{N_u} \alpha_\nu A^\nu \int_0^{T_f} P(t)P(t-\Delta)dt, \tag{16}$$

where Δ is the time difference between the different users expressed as

$$\Delta = (C_j^1 - C_j^\nu)T_C + (d_j^\nu - \delta_j) + (\tau^\nu - \tau^1). \tag{17}$$

If the correlation function of the pulse $P(t)$ is defined by

$$h(\Delta) = \int_0^{T_f} P(t)P(t-\Delta)dt, \tag{18}$$

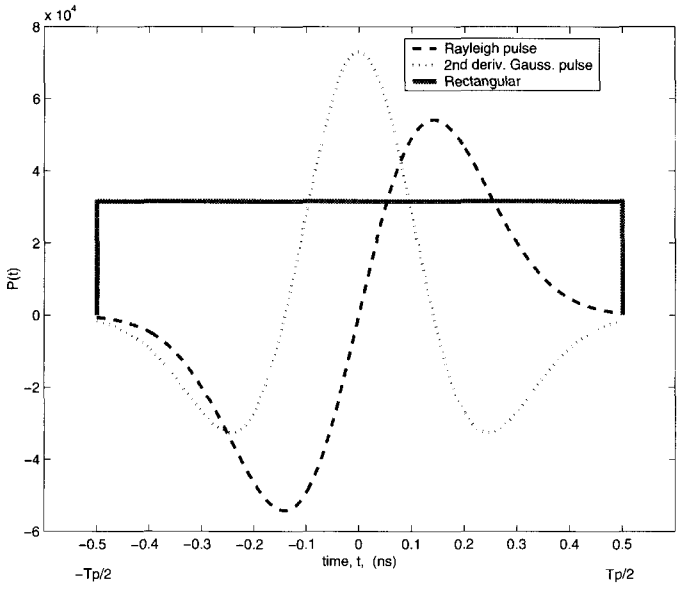

Fig. 5. UWB pulses with $T_P = 1$ ns.

then the expression for MAI in (16) can be written as

$$NI = \sum_{\nu=2}^{N_u} \alpha_\nu A^\nu h(\Delta). \tag{19}$$

It is assumed that all the time-hopping code elements C_j are random and independent, with uniform distribution over frame interval T_f for all users and frames. Each user has a uniformly distributed data source. The time delays are also assumed random, i.i.d. uniformly distributed over the frame interval. Under the assumptions listed above, and noting that MAI pulses of interest fall within the same UWB frame, the time difference Δ is a uniformly distributed random variable over the interval $[-T_f, T_f]$.

Various waveforms with complex mathematical formats have been proposed for impulse radio including Gaussian pulse, Gaussian monocycle [1], and Rayleigh monocycle [8]. All of these waveforms reflect the high-pass filtering impact of the transmitter and receiver antennas. To simplify our calculation, we consider three types of waveforms, namely, Rectangular, Rayleigh and the 2nd derivative Gaussian pulses. The considered waveforms are presented in Fig. 5 with $T_P = 1$ ns. This analysis can be extended to other waveforms.

We assume the following *rectangular waveform*

$$P_{rect}(t) = \begin{cases} \sqrt{\frac{1}{T_P}}, & 0 \le t \le T_P \\ 0, & otherwise \end{cases}. \tag{20}$$

The correlation function $h(\Delta)$ for $P_{rect}(t)$ in (20) is

$$h_{rect}(\Delta) = \begin{cases} 1 - \frac{|\Delta|}{T_P}, & 0 \le |\Delta| \le T_P \\ 0, & otherwise \end{cases}. \tag{21}$$

Comparing with a rectangular waveform, the main characteristic of monocycle signal is that they have a zero DC component

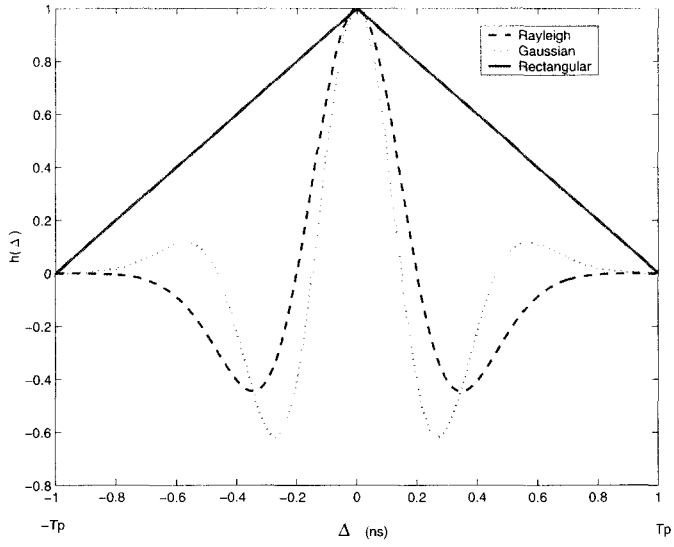

Fig. 6. Autocorrelation of UWB waveforms with $T_P = 1$ ns.

to allow them radiate effectively. The normalized *2nd derivative Gaussian pulse* is expressed as

$$P_{2nd\ gauss}(t) = \sqrt{\frac{8}{3\varepsilon}}\left[1 - 4\pi\left(\frac{t}{\varepsilon}\right)^2\right] e^{-2\pi\left(\frac{t}{\varepsilon}\right)^2}, \quad (22)$$

where ε is a time scale factor and its relation to pulse width T_P is $T_P = 7\varepsilon$ which contains 99.99% of the total energy. The corresponding autocorrelation function is found to be as

$$h_{2nd\ gauss}(\Delta) = \left[1 - 4\pi\left(\frac{\Delta}{\varepsilon}\right)^2 + \frac{4\pi^2}{3}\left(\frac{\Delta}{\varepsilon}\right)^4\right] e^{-\pi\left(\frac{\Delta}{\varepsilon}\right)^2}. \quad (23)$$

The normalized Rayleigh pulse is expressed as

$$P_{ray}(t) = \sqrt{\frac{8\varepsilon}{\sqrt{2\pi}}}\frac{t}{\varepsilon^2} e^{-\left(\frac{t}{\varepsilon}\right)^2}, \quad (24)$$

and its autocorrelation function is found to be as

$$h_{ray}(\Delta) = \left[1 - \left(\frac{\Delta}{\varepsilon}\right)^2\right] e^{-\frac{1}{2}\left(\frac{\Delta}{\varepsilon}\right)^2}, \quad (25)$$

Fig. 6 shows the autocorrelation functions of the considered waveforms

III. PERFORMANCE ANALYSIS

For simplicity, and without loss of generality, we assume that signals are transmitted in the l-th time slot. With perfect synchronization, channel delay τ^1 is known, the time hopping sequence C_j^1 is known, and the decision variables are

$$U_i = \begin{cases} U_l : \alpha^1 A^1 + NI + N, & i = l \\ U_p : NI + N, & i = 1, \cdots, M, i \neq l \end{cases}. \quad (26)$$

It is known that the MAI is not Gaussian. However, we assume large number of users to justify the Gaussian assumption for MAI by invoking the central limit theorem. The decision variables are independent Gaussian random variables distributed as follows:

$$\begin{aligned} U_l &: N\left(\alpha^1 A^1 + E[NI] + E[N], \sigma_{NI}^2 + Var(N)\right) \\ U_p &: N\left(E[NI] + E[N], \sigma_{NI}^2 + Var(N)\right). \end{aligned} \quad (27)$$

where $N(0,1)$ denotes the Gaussian distribution with zero mean and unit variance, and $E(x)$ and $Var(x)$ are the mean and variance of x, respectively.

The mean $E(N)$ and variance $Var(N)$ are found to be 0 and $N_0/2$, respectively. The corresponding parameters for MAI are found to be

$$E[NI] = \sum_{\nu=2}^{N_u} E[\alpha_\nu] A^\nu E[h(\Delta)], \quad (28)$$

and

$$\sigma_{NI}^2 = \sum_{\nu=2}^{N_u} (A^\nu)^2 \cdot \left(E[\alpha_\nu^2]E[h^2(\Delta)] - E^2[\alpha_\nu]E^2[h(\Delta)]\right). \quad (29)$$

The mean of $h(\Delta)$ can be calculated as follows:

i) For rectangular waveform

$$\begin{aligned} E[h(\Delta)] &= E[h_{rect}(\Delta)] \\ &= \int_{-T_P}^{T_P} h_{rect}(\Delta)\frac{1}{2T_f} d\Delta = \frac{1}{2\beta}. \end{aligned} \quad (30)$$

ii) For the 2nd derivative Gaussian waveform

$$\begin{aligned} E[h_{2nd\ gauss}(\Delta)] = \frac{2}{\beta}\frac{\varepsilon}{2T_P}&\left(\frac{1}{\pi} - 1\right) erf\left(\sqrt{\pi}\frac{T_P}{\varepsilon}\right) \\ &+ \left(2 - 2\left(\frac{T_P}{\varepsilon}\right)^2 - \frac{1}{\pi}\right) exp\left(-\pi\left(\frac{T_P}{\varepsilon}\right)^2\right), \end{aligned} \quad (31)$$

where $erf(\cdot)$ is the error function [7].

iii) For Rayleigh waveform

$$E[h_{ray}(\Delta)] = \frac{1}{\beta} e^{-\frac{1}{2}\left(\frac{T_P}{\varepsilon}\right)^2}. \quad (32)$$

The 2nd moment of $h(\Delta)$, $E[h^2(\Delta)]$, is calculated as follows:

i) For rectangular waveform

$$\begin{aligned} E[h^2(\Delta)] &= E[h_{rect}^2(\Delta)] \\ &= 2\int_0^{T_P} h_{rect}^2(\Delta)\frac{1}{2T_f} d\Delta = \frac{1}{3\beta}. \end{aligned} \quad (33)$$

ii) For the 2nd derivative Gaussian waveform

$$E[h^2_{2nd\,gauss}(\Delta)] = \frac{2\varepsilon}{T_P\beta}\left[\frac{1}{\sqrt{2}}\left(1-\frac{1}{\pi}+\frac{35}{96\pi^2}\right)erf\left(\sqrt{2\pi}\frac{T_P}{\varepsilon}\right) + \left(\left(-1-\frac{35}{48\pi^2}+\frac{2}{\pi}\right)\frac{T_P}{\varepsilon} + \left(\frac{8}{3}-4\pi-\frac{35}{36\pi}\right)\left(\frac{T_P}{\varepsilon}\right)^3 + \left(-\frac{7}{9}+\frac{8}{3}\pi\right)\left(\frac{T_P}{\varepsilon}\right)^5 - \frac{4}{9}\pi\left(\frac{T_P}{\varepsilon}\right)^7\right)e^{-2\pi(\frac{T_P}{\varepsilon})^2}\right]. \quad (34)$$

iii) For Rayleigh waveform

$$E[h^2_{ray}(\Delta)] = \frac{1}{4\beta}\left[\left(1-\left(\frac{T_P}{\varepsilon}\right)^2\right)e^{-(\frac{T_P}{\varepsilon})^2} + \frac{3\sqrt{\pi}}{2}\frac{T_P}{\varepsilon}erf\left(\frac{T_P}{\varepsilon}\right)\right]. \quad (35)$$

If $T_P/\varepsilon = 7$, (31), (34), (32), and (35) can be reduced to:

$$E[h_{2nd\,guass}(\Delta)] = \frac{-9.738\times10^{-2}}{\beta},$$

$$E[h^2_{2nd\,guass}(\Delta)] = \frac{0.14519}{\beta},$$

$$E[h_{ray}(\Delta)] = \frac{2.29\times10^{-11}}{\beta},$$

and

$$E[h^2_{ray}(\Delta)] = \frac{0.095}{\beta}.$$

The *pdf* for decision variable U_l can be represented as

$$p(U_l) = \frac{1}{\sqrt{2\pi}\sigma_l}e^{-\frac{(U_l-\mu_l)^2}{2\sigma_l^2}}, \quad (36)$$

where $\mu_l = \alpha^1 A^1 + E[NI]$ and $\sigma_l = \sqrt{\sigma^2_{NI}+\frac{N_0}{2}}$. The *pdf* for decision variable U_p can be expressed as

$$p(U_p) = \frac{1}{\sqrt{2\pi}\sigma_p}e^{-\frac{(U_p-\mu_p)^2}{2\sigma_p^2}}, \quad (37)$$

where $\mu_p = E[NI]$ and $\sigma_p = \sigma_l = \sqrt{\sigma^2_{NI}+\frac{N_0}{2}}$.

The conditional probability of correct decision is

$$P_{C|U_l} = prob(U_l > U_1, \cdots, U_l > U_i, \cdots, U_l > U_M | U_l, l \neq i), \quad (38)$$

and the average probability of correct decision is

$$P_C = \int_{-\infty}^{\infty}[prob(U_l > U_i)|U_l, l \neq i)]^{M-1}p(U_l)dU_l, \quad (39)$$

by substituting (36) and (37) into (39), and after some calculus with the substitution $x = \frac{U_l-\mu_l}{\sqrt{2}\sigma}$, the probability of correct decision becomes

$$P_C = \frac{1}{\sqrt{\pi}2^{M-1}}\int_{-\infty}^{\infty}\left[1+erf\left(x+\frac{\alpha^1A^1}{\sqrt{2}\sigma}\right)\right]^{M-1}\cdot e^{-x^2}dx, \quad (40)$$

where σ is defined as

$$\sigma = \sqrt{\frac{N_0}{2}+\sum_{\nu=2}^{N_\nu}(A^\nu)^2(E[\alpha_\nu^2]E[h^2(\Delta)] - E^2[\alpha_\nu]E^2[h(\Delta)])}. \quad (41)$$

Under perfect power control assumptions, i.e., $A^\nu = A^1 = A$, $E^2[\alpha_\nu] = E^2[\alpha]$ and $E[\alpha_\nu^2] = E[\alpha^2]$ for all ν, the term $\frac{\alpha^1A^1}{\sqrt{2}\sigma}$ in (40) can be expressed as

$$\frac{\alpha^1A^1}{\sqrt{2}\sigma} = \sqrt{\frac{\gamma\frac{E_P}{N_0}}{1+(N_u-1)2\left(\frac{E_P}{N_0}\right)(E[\alpha^2]E[h^2(\Delta)] - E^2[\alpha]E^2[h(\Delta)])}}, \quad (42)$$

where $E_P = \sqrt{A}$ is the pulse energy and $\frac{E_P}{N_0}$ is the pulse energy to noise ratio. The probability of symbol error is $P_S = 1 - P_C$.

A. AWGN Channel

In Gaussian channel, the channel attenuation factor can be assumed as unity, $\alpha = 1$, and the average probability of correct decision error can be reduced as (43) as shown at the bottom of next page. This integration is evaluated by Hermite integration method [7] as (44) shown at the bottom of next page. In (44), x_i is the i-th zero of the n-th order Hermite polynomial $H_n(x)$ and w_i is a weight defined by $\frac{2^{n-1}n!\sqrt{\pi}}{n^2[H_n(x_i)]^2}$. Numerical values for x_i and w_i are given by [7].

The term $(E[h^2(\Delta)] - E^2[h(\Delta)])$ in (44) represents the variance of the autocorrelation function denoted by σ_h^2. From (30) and (33) for $\beta > 100$, the parameter σ_h^2 for rectangular pulse can be approximated by

$$\sigma_h^2(rect) = \frac{1}{3\beta} - \frac{1}{4\beta^2} \approx \frac{0.333}{\beta}, \quad (45)$$

and the corresponding parameters for the 2nd derivative Gaussian and Rayleigh waveforms with $T_P/\varepsilon = 7$ are

$$\sigma_h^2(2ndgauss) = \frac{0.14519}{\beta} - \frac{9.48368\times10^{-3}}{\beta^2} \approx \frac{0.14519}{\beta}, \quad (46)$$

and

$$\sigma_h^2(ray) = \frac{0.095}{\beta} - \frac{5.242 \times 10^{-22}}{\beta^2} \approx \frac{0.095}{\beta}. \quad (47)$$

From (43) and by comparing (45), (46), and (47), we clearly observe that the monocycle waveforms is beneficial in reducing the MAI. Finally, the probability of symbol error is again given by $P_{S(AWGN)} = 1 - P_{C(AWGN)}$.

B. Rician Fading Channel

To evaluate the system performance in terms of probability of correct decision, we substitute (42) into (40), and average P_C over the non-central Chi-square distribution for γ defined by (3). The average probability of correct decision is

$$\bar{P}_{C(Rician)} = \frac{e^{-K}}{\sqrt{\pi}2^{M-1}} \cdot \int_0^\infty \int_{-\infty}^\infty \left[1 + erf\left(x + \sqrt{\frac{u\frac{E_P}{N_0}}{(1+K)\zeta}}\right)\right]^{M-1} \cdot e^{-x^2} e^{-u} I_0(2\sqrt{Ku}) dx du, \quad (48)$$

where $\zeta = 1 + (N_u - 1)2(\frac{E_P}{N_0})(E[\alpha^2]E[h^2(\Delta)] - E^2[\alpha] \cdot E^2[h(\Delta)])$. The integrations in (48) are evaluated using Laguerre and Hermite integration methods described in [7] as follows:

$$\bar{P}_{C(Rician)} = \frac{e^{-K}}{\sqrt{\pi}2^{M-1}} \sum_{i=1}^{n_2} w_i \sum_{j=1}^{n_1} \nu_j I_0(2\sqrt{Ku_j}) \cdot \left[1 + erf\left(x_i + \sqrt{\frac{u_j\frac{E_P}{N_0}}{(1+K)\zeta}}\right)\right]^{M-1}, \quad (49)$$

where u_j is the j-th zero of the n_1-th order Laguerre polynomial $L_{n_1}(u)$ and ν_j is a weight defined by $\frac{(n_1!)^2 u_j}{(n_1+1)^2[L_{n_1+1}(u_j)]^2}$. Numerical values for u_j and ν_j are given by [6]. The parameters x_i, w_i, and n_2 are defined earlier in (44).

The probability of symbol error is $P_{S(Rician)} = 1 - P_{C(Rician)}$. The performance expressions found are very general and can be used for Rayleigh and Rician channels for different pulse shapes.

C. Nakagami Fading Channel

To evaluate the performance of M-ary PPM UWB system in Nakagami fading channels, we substitute (42) into (40), and average P_C over the Gamma distribution for γ defined by (6). The average probability of correct decision is

$$\bar{P}_{C(Nakagami)} = \frac{1}{\Gamma(m)\sqrt{\pi}2^{M-1}} \cdot \int_0^\infty \int_{-\infty}^\infty \left[1 + erf\left(x + \sqrt{\frac{u\frac{E_P}{N_0}}{m\zeta}}\right)\right]^{M-1} \cdot u^{m-1} e^{-x^2-u} dx du, \quad (50)$$

where ζ is defined in (48). The integrations in (50) are evaluated using Laguerre and Hermite integration methods described in [7] as follows:

$$\bar{P}_{C(Nakagami)} = \frac{1}{\Gamma(m)\sqrt{\pi}2^{M-1}} \sum_{i=1}^{n_2} w_i \sum_{j=1}^{n_1} \nu_j u_j^{m-1} \cdot \left[1 + erf\left(x_i + \sqrt{\frac{u_j\frac{E_P}{N_0}}{m\zeta}}\right)\right]^{M-1}, \quad (51)$$

where u_j, ν_j , and $n - 1$ are defined earlier in (49) and x_i, w_i, n_2 are defined in (44).

The probability of symbol error is $P_{S(Nakagami)} = 1 - P_{C(Nakagami)}$. The performance expressions found are very general and can be used for Rayleigh and Nakagami channels for various waveforms.

IV. NUMERICAL RESULTS

Figs. 7–9 depict the effect of pulse selection on the user SER of M-ary PPM UWB in Rician and Nakagami fading and AWGN channels. It is obvious that the monocycle pulses represented by the 2nd derivative Gaussian and Rayleigh pulses outperform the rectangular pulse regardless of the channel. This is due to the autocorrelation properties of the monocycle pulses. One can also observe that the performance is slightly degraded with increased M for monocycle pulses. This suggests higher spectral efficiency.

Using the Rayleigh pulse at SER-level of 10^{-3}, the performance differences between $M = 2$ and $M = 8$ are approximately 1.7 dB, 3.8 dB and 3.4 dB in AWGN, Rician and Nakagami channels, respectively. The corresponding values for the 2nd Gaussian pulse are 4.5 dB, 6.5 dB and 5.6 dB, respectively. Using the rectangular pulse, the system performance saturates before the SER-level of 10^{-3} is achieved. Due to the larger distance between the modulation points, the lower level modulation ($M = 2$) outperforms the higher ones ($M = 8$). Note that the values of $K = 10$ and $m = 5$ were selected to show the accura-

$$P_{C(AWGN)} = \frac{1}{2^{M-1}} \int_{-\infty}^\infty \left[1 + erf\left(x + \sqrt{\frac{\frac{E_P}{N_0}}{1 + (N_u - 1)2\left(\frac{E_P}{N_0}\right)(E[h^2(\Delta)] - E^2[h(\Delta)])}}\right)\right]^{M-1} e^{-x^2} dx. \quad (43)$$

$$P_{C(AWGN)} = \frac{1}{2^{M-1}} \sum_{i=1}^{n} w_i \left[1 + erf\left(x_i + \sqrt{\frac{\frac{E_P}{N_0}}{1 + (N_u - 1)2\left(\frac{E_P}{N_0}\right)(E[h^2(\Delta)] - E^2[h(\Delta)])}}\right)\right]^{M-1} e^{-x^2}. \quad (44)$$

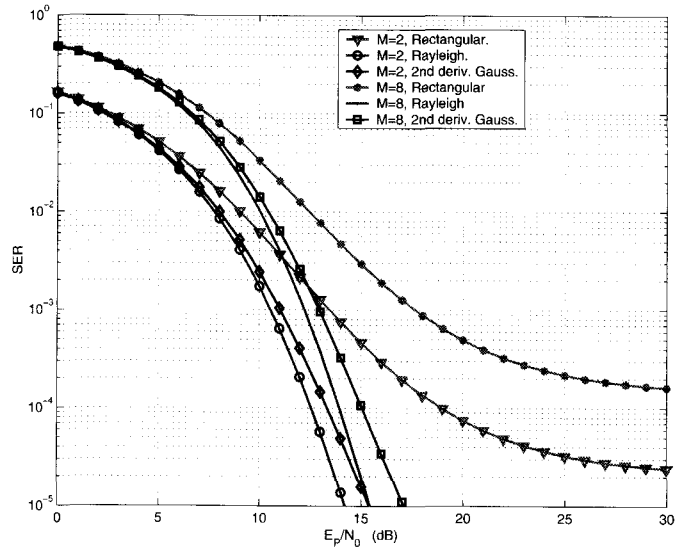

Fig. 7. User SER for multiuser M-ary PPM UWB radio system with $N_u = 10$ users, spreading ratio β =100, and $T_P/\varepsilon = 7$, in AWGN channel.

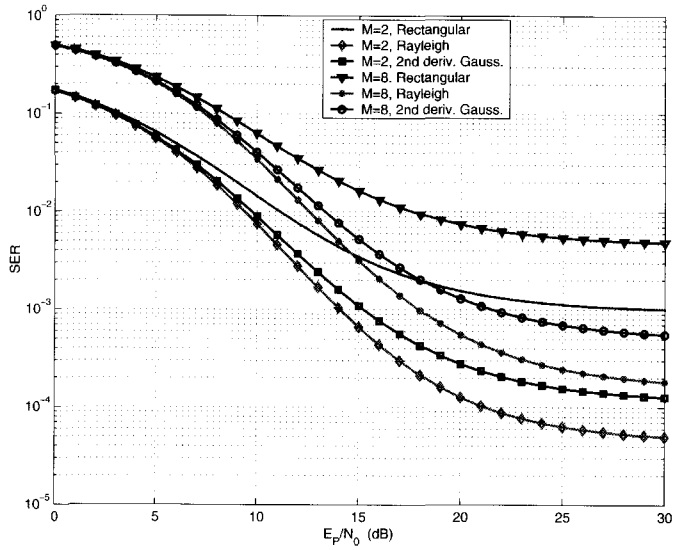

Fig. 8. User SER for multiuser M-ary PPM UWB radio system with $N_u = 10$ users, spreading ratio $\beta = 100$, and $T_P/\varepsilon = 7$, in Rician fading channel with $K = 10$.

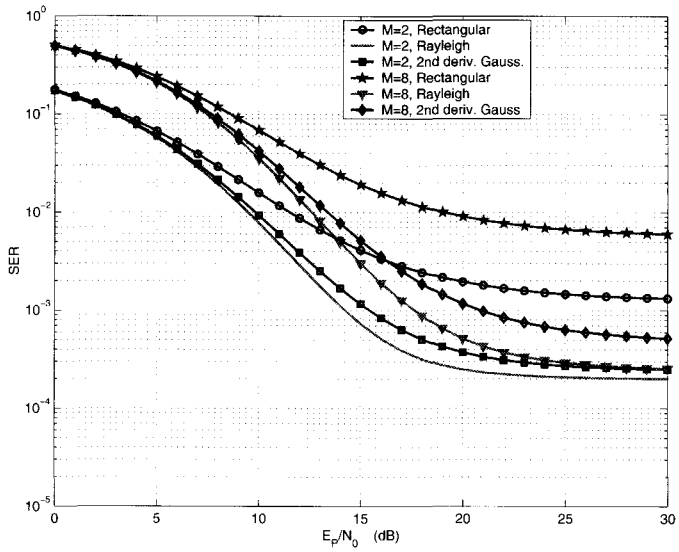

Fig. 9. User SER for multiuser M-ary PPM UWB radio system with $N_u = 10$ users, spreading ratio $\beta = 100$, and $T_P/\varepsilon = 7$, in Nakagami fading channel with $m = 5$.

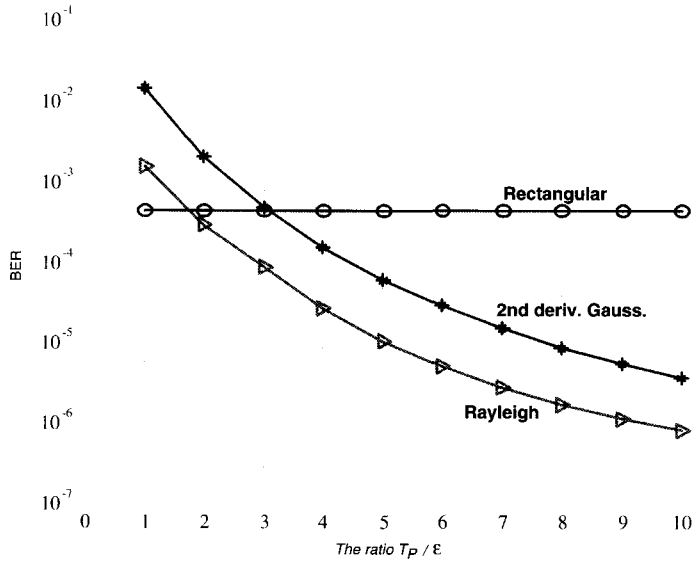

Fig. 10. User BER for multiuser 2-ary PPM UWB radio system with $N_u = 10$ users, spreading ratio $\beta = 100$, $E_P/N_0 = 15$ dB, in AWGN channel.

cy of the relationship between the Rician and Nakagami distributions. It is obvious that such relation holds in most of the presented results.

In the simulations, the pulse shaping ratio T_P/ε for both the 2nd derivative Gaussian and Rayleigh pulses was loosely selected to be equal to 7. This selection may degrade the performance of the 2nd derivative Gaussian pulse as compared to that of Rayleigh pulse.

It is clear that the pulse shaping ratio is of importance that may influence the system SER performance. Figs. 10-12 depict the effect of pulse shaping ratio, on the performance of M-ary PPM UWB system. These figures suggest that the shaping ratio must be greater than 2 and 3 for Rayleigh pulses and the 2nd derivative Gaussian pulses, respectively. Moreover, the performance with Rayleigh pulses can be made equal to that with the 2nd derivative Gaussian pulse by an appropriate pulse shaping ratio.

The effect of system capacity on the BER is presented in Figs. 13 and 14. We observed that practical pulses such as monocycle pulses provide higher capacity than ideal ones. For the same BER, the number of accommodated users in the system can be significantly increased using the 2nd derivative Gaussian pulse. The difference in the performance as a function of simultaneous users between the Rician and Nakagami channels is insignificant. This analysis can also be extended to the other UWB waveforms. With $K = 10$ and $m = 5$, the results of Figs. 13 and 14 are similar because of the validity of the relationship between the Rician and Nakagami channels.

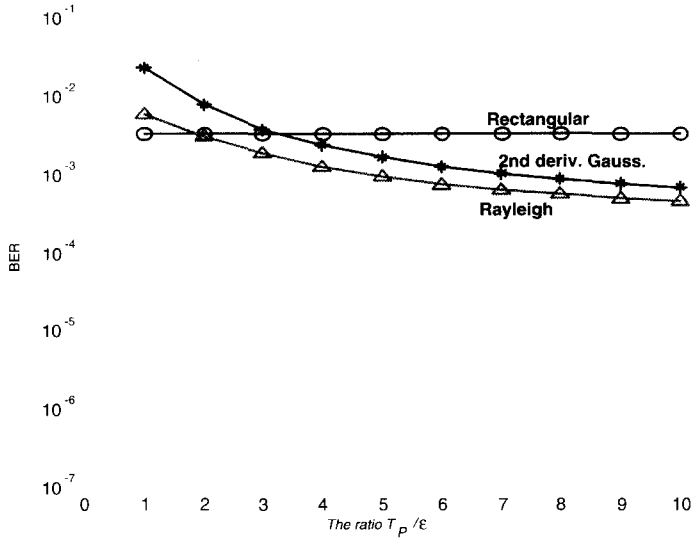

Fig. 11. User BER for multiuser 2-ary PPM UWB radio system with $N_u = 10$ users, spreading ratio $\beta = 100$, $E_P/N_0 = 15$ dB, in Rician fading channel with $K = 10$.

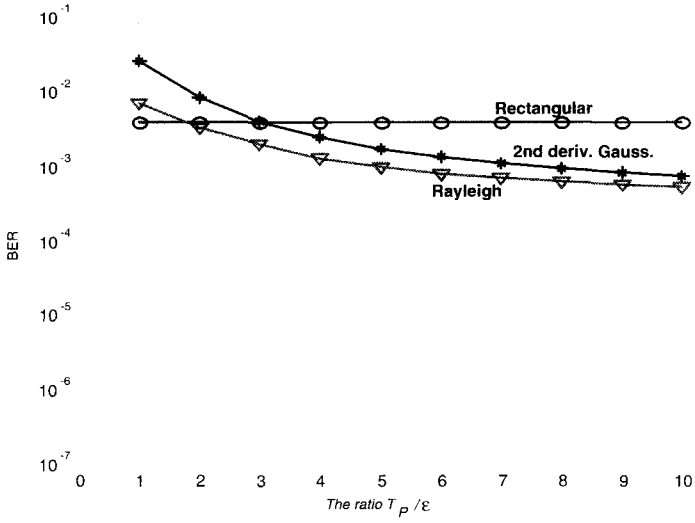

Fig. 12. User BER for multiuser 2-ary PPM UWB radio system with $N_u = 10$ users, spreading ratio $\beta = 100$, $E_P/N_0 = 15$ dB, in Nakagami fading channel with $m = 5$.

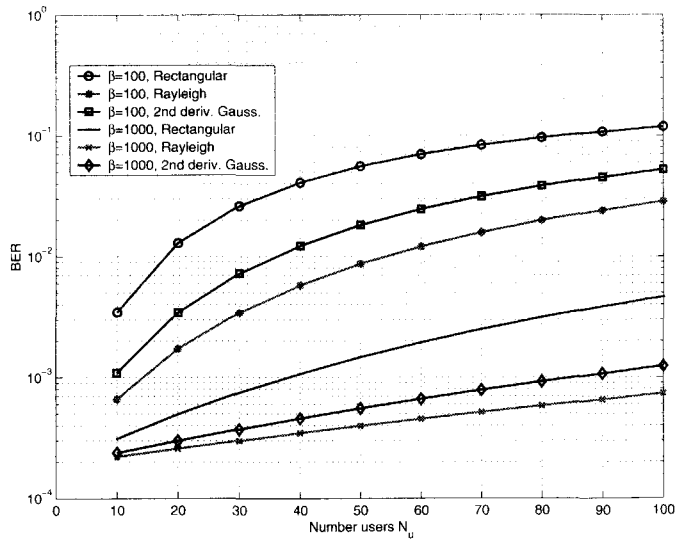

Fig. 13. User BER with respect to number of users and spreading ratio, β, for multiuser 2-ary PPM UWB radio system with $E_b/N_0 = 15$ dB in Rician fading channel with $K = 10$.

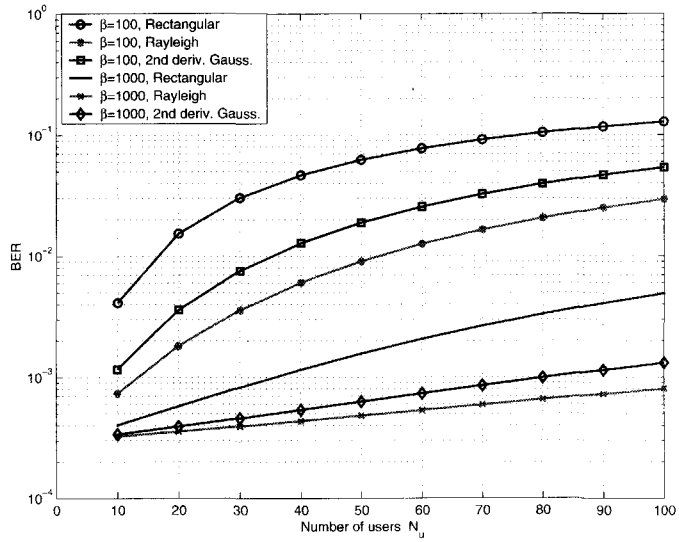

Fig. 14. User BER with respect to number of users and spreading ratio, β, for multiuser 2-ary PPM UWB radio system with $E_b/N_0 = 15$ dB in Nakagami fading channel with $m = 5$.

V. CONCLUSIONS

In this paper, we have investigated the SER performance of coherent M-ary PPM UWB multiple-access system in Rician and Nakagami fading channels. Among many practical pulse waveforms, rectangular, the 2nd derivative Gaussian and Rayleigh pulses were considered. Closed form expressions for SER were derived using M-ary PPM UWB system for AWGN, Rician and Nakagami fading channels. The expressions are generalized in such a way that it can be applied to multiuser UWB environment using various pulse waveforms. Monocycle pulse is found to be much more robust against MAI than rectangular pulse even in fading channels. Moreover, the system capacity with monocycle pulses would be improved compared with rectangular pulse in fading channels. The results also showed that the performance of the rectangular pulse may decrease rapidly as a response to changes in channel statistics. For example, SER-level of 10^{-3} cannot be achieved for both Rician and Nakagami channels. The performance with Rayleigh pulse is about 1 dB superior to that with the 2nd derivative Gaussian pulse for the same SER-level in all the studied channels. Although the system performance degrades for increased M for all the studied cases, the degradation is minimal with the monocycle pulses. This work may be extended to account for multipath fading using a suitable UWB receiver.

ACKNOWLEDGEMENT

This work is performed as part of the framework project ULTRAWAVES under contract IST-2001-35189 to the European Community.

REFERENCES

[1] M. Win and R. Scholtz, "Ultra-wide bandwidth time-hopping spread-spectrum impulse radio for wireless multiple-access communications," *IEEE Trans. Commun.*, vol. 48, no. 4, pp. 679–691, Apr. 2000.

[2] Federal Communications Commission, "First Report and Order", FCC 02-48, 2002.

[3] J. R. Foerster, "The effects of multipath interference on the performance of UWB systems in an indoor wireless channel," in *Proc. IEEE VTC'2001*, Spring 2001, pp. 1176–1180.

[4] L. Ge, G. Yue, and S. Affes, "On the BER performance of pulse-position-modulation UWB radio in multipath channels," in *Proc. IEEE Conf. Ultra Wideband Sys. and Technol.*, May 2002, pp. 231–234.

[5] M. Abdel-Hafez, F. Alagöz, and M. Hämäläinen, "M-ary PPM UWB radio in fading channels," in *Proc. IEEE MWCN'2003*, Singapore, Oct. 2003, pp. 253–257.

[6] V. Hovinen, M. Hämäläinen, and T. Patsi, "Ultra wideband indoor radio channel models: Preliminary results," in *Proc. IEEE Conf. Ultra Wideband Sys. and Technol.*, May 2002, pp. 75–79.

[7] M. Abramowitz and A. S. Irene, *Handbook of Mathematical Functions*, Dover Publications, Inc. New York, Dec. 1972.

[8] J. T. Conroy, J. L. LoCicero, and D. R. Ucci, "Communication techniques using monopulse waveforms," in *Proc. IEEE MILCOM' 99*, vol. 2, 1999, pp. 1191–1185.

[9] J. G. Proakis, *Digital Communications*, 3rd edition, McGRAW-HILL, 1995.

[10] N. Nakagami, "The m-distribution, a general formula for intensity distribution of rapid fading," *Statistical Methods in Radio Wave Propagation*, W. G. Hoffman, ed., pp. 3-36, Oxford, England: Pergamon, 1960.

[11] S. A. Abbas and A. U. Sheikh, "A geometric theory of Nakagami fading multipath mobile radio channel with physical interpretations," in *Proc. VTC'96*, vol. 2, Atlanta, USA Apr. 28–May 1 1996, pp. 637–641.

Mohammed Abdel-Hafez was born in Qalqilia, Palestine. He received his B.Sc, M.Sc, and Ph.D degrees all in Electrical and Electronic Engineering from Eastern Mediterranean University, Northern Cyprus, Turkey in 6/1992, 8/1994, and 11/1997, respectively. From 1992 to 1997 he was a Research Engineer at Department of Electrical and Electronic Engineering, EMU, Turkey. During the year 1995, he was an instructor at Jerusalem University, Department of Electrical Engineering. From 1997 to 1999 he was with Palestine Telecommunication Company (PALTEL) as data communication section manager. In August 1999, he joined Centre for Wireless Communications at the University of Oulu as senior research scientist and project manager. He is currently assistant professor of Electrical Engineering at United Arab Emirates University in United Arab Emirates. He is a frequent visiting professor at Oulu University, Centre for Wireless Communications, Oulu, Finland. His research of interests includes performance analysis of mobile communication systems, future broadband wireless systems, and Wireless LAN, Multicarrier CDMA, and Ultra Wide Band (UWB) systems. Dr. Abdel-Hafez has published more than 35 conference or journal papers in the field of wireless communications and digital signal processing

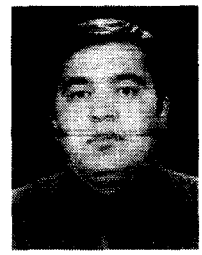

Fatih Alagöz is an assistant professor in and chairman of the Department of Electrical and Electronics Engineering, Harran University, Turkey. He received his B.Sc. in electrical engineering in 1992, from the Middle East Technical University, Turkey. During 1993, he was a research engineer in a missile manufacturing company, Muhimmatsan AS, Turkey. He obtained his M.Sc. and D.Sc. degrees both in electrical engineering in May 1995 and January 2000, respectively, from the George Washington University, USA. During 2001 -2003, he was with the Department of Electrical Engineering, United Arab Emirates University, UAE. His research interests are in the areas of wireless/mobile/satellite networks, teletraffic modeling, performance evaluation and modeling of terrestrial and satellite mobile communications, neural networks, and multi-user detection. He has edited two books, and published more than thirty scholarly papers in selected journals and conferences. Dr Alagoz is a Member of IEEE, and Satellite and Space Communications Technical Committee. He has numerous awards including the YOK Scholarship achieved based on a nationwide selection examination, and the ACM MSWIM'99 Best Paper Award.

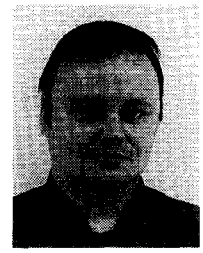

Matti Hämäläinen was born in Sodankyla, Finland in 1967. He received his Master of Science (in Electrical Engineering) and Licentiate of Technology degrees from the University of Oulu, Oulu, Finland in 1994 and 2002, respectively. He joined Telecommunication Laboratory, University of Oulu at 1993. Since 1999 he has been with Centre for Wireless Communications at University of Oulu as a researcher and a project manager. Currently he is also a Dr.Tech. student at the same university. His research interests are wideband radio channel modeling, spread spectrum communications and ultra wideband systems.